

High-resolution spectroscopy of *ROSAT*-discovered weak-line T Tauri stars near Lupus

R. Wichmann,^{1,3} E. Covino,² J. M. Alcalá,^{2,6} J. Krautter,³ S. Allain⁴ and P. H. Hauschildt⁵

¹*IUCAA, Post Bag 4, Ganeshkhind, Pune 411007, India*

²*Osservatorio Astronomico di Capodimonte, Napoli, Italy*

³*Landessternwarte Königstuhl, D-69117 Heidelberg, Germany*

⁴*Laboratoire d'Astrophysique, Observatoire de Grenoble, Université Joseph Fourier, B.P.53, F-38041 Grenoble Cedex 9, France*

⁵*University of Georgia, Athens, GA 30602-2451, USA*

⁶*Instituto Nacional de Astrofísica, Óptica y Electrónica, A.P. 51 y 216, C.P. 72000, Puebla, México*

Accepted 1999 March 22. Received 1999 March 11; in original form 1998 August 14

ABSTRACT

We present high-resolution optical echelle spectroscopy for a large fraction of the Li-rich late-type stars recently discovered in the vicinity of the Lupus dark clouds. Our results confirm the high Li I $\lambda 6708$ equivalent widths previously estimated from medium-resolution spectra, thus adding strength to the conclusion that the large majority of these stars are still in the pre-main-sequence phase of their evolution, contrary to claims from other authors that many of them might be zero-age main-sequence stars. We present a statistical approach to derive a mean distance for the sample, and find that it is consistent with, or slightly lower than, the *Hipparcos* distance of the Lupus star-forming region. The radial velocities measured for part of these stars are consistent with those observed for the Lupus star-forming region, while stars outside the dark clouds show a mean difference of the order of 3 km s^{-1} . The projected rotational velocities show a lack of slow rotators, which is interpreted as a consequence of the X-ray selection of the sample. The Li-rich stars in Lupus studied in this work yield a fairly ‘clean’ sample of very young stars, while in other star-forming regions a larger fraction of older zero-age main-sequence stars has been found among *ROSAT*-discovered Li-rich stars. We argue that this fact reflects the relation of these stars with the Gould Belt.

Key words: stars: distances – stars: late-type – stars: pre-main-sequence – ISM: individual: Lupus.

1 INTRODUCTION

In recent years, follow-up optical spectroscopic observations of X-ray sources detected in and around nearby star-forming regions (SFRs) by the *ROSAT* All-Sky Survey (RASS) have revealed large numbers of Li-rich late-type stars (Wichmann et al. 1996; Alcalá et al. 1995, 1996; Neuhäuser et al. 1995; Krautter et al. 1997). Henceforth we will refer to these papers as the RASS papers. Owing to their large Li I $\lambda 6708$ equivalent width, as measured in medium-resolution ($\sim 4 \text{ \AA}$) spectra, as well as to their location near to well-known SFRs, it has been presumed in the RASS papers that these stars are associated with the respective SFRs, and comprise a population of weak-line T Tauri stars (WTTSS) with ages ranging from those of optically discovered TTSs (10^5 –few 10^6 yr) up to a few 10^7 yr (Wichmann et al. 1997a). Thus, for convenience we will henceforth denote these stars as *ROSAT* WTTSS, although in this work some of them will be identified as older, namely zero-age main-sequence (ZAMS) stars.

The aforementioned interpretation has provoked some criticism from a few authors, who argued that the number of Li-rich stars

discovered was consistent with an ubiquitous foreground population of dispersed ZAMS stars (Briceño et al. 1997), and that, from comparison with results for *Einstein* Extended Medium Sensitivity Survey (EMSS) sources, one might expect most of the *ROSAT* WTTSS to be ZAMS stars (Micela, Favata & Sciortino 1997). Clearly, more observational constraints on the nature of the *ROSAT* WTTSS are required.

In a recent study, Wichmann et al. (1997b) showed that the spatial distribution of *ROSAT* WTTSS near Lupus, perpendicular to the galactic plane, is centred on the Gould Belt (Gould 1879; for a recent review of the Gould Belt see Pöppel 1997). It is therefore incompatible with the Briceño et al. (1997) model, which would predict these stars to be centred on the galactic plane. This represents strong evidence that these stars – like the Lupus dark clouds themselves – are part of the Gould Belt rather than pertaining to the ubiquitous dispersed ZAMS population, postulated by Briceño et al. (1997).

We have obtained high-resolution ($R \sim 20\,000$ – $34\,000$) optical echelle spectra of a major fraction of the *ROSAT* WTTSS in Lupus (Krautter et al. 1997). These data allow us to study radial

Table 1. Results from echelle spectroscopy. We list designation, apparent Cousins I magnitude I_C (Wichmann et al. 1997a), spectral type SpT (Krautter et al. 1997), equivalent widths W_{Li} , ΔW_{Li} (see text for definition) and $W_{\text{H}\alpha}$, as well as the type of $\text{H}\alpha$ profile $P_{\text{H}\alpha}$ ('m' means multiple), $V \sin i$ from cross-correlation (CC) and from the Fourier transform method (FFT), the radial velocity V_{RAD} , and the observatory/instrument OB (1: ESO/CASPEC, 2: CTIO/Echelle). For the four stars with $V \sin i > 100$, and the two S2 observed with CASPEC, W_{Li} is an upper limit only. I magnitudes and SpT for Sz 77, 82, 96, and 129 are from Hughes et al. (1994). Stars pertaining to the 'on-cloud' sample are marked by the superscript 'p'.

Designation	I_C [mag]	SpT	W_{Li} [Å]	ΔW_{Li} [Å]	$W_{\text{H}\alpha}$ [Å]	$P_{\text{H}\alpha}$	$V \sin i_{\text{CC}}$ [km s $^{-1}$]	$V \sin i_{\text{FFT}}$ [km s $^{-1}$]	V_{RAD} [km s $^{-1}$]	OB
RXJ1507.2–3505	9.57	K0	0.324	0.016	2.59	Ia	15.0		1.4	2
RXJ1507.6–4603	10.52	K2	0.401	0.058	−0.36	II-C	12.8		11.1	1
RXJ1507.9–4515	9.98	G3	0.048	−0.150	2.70	Ia	31.1	13.0	21.1	1
RXJ1508.6–4423	9.83	G8	0.386		−0.55	II-C	109.2	125.0	4.6	1
RXJ1508.7–4400	9.56	G7	0.278	0.054	2.87	Ia	24.4	24.0	6.6	1
RXJ1511.6–3550	11.21	K5	0.387	0.049	−0.14	II-C	10.0	11.0	2.2	2
RXJ1514.0–4629A	12.15	M2	0.380	0.239	−1.57	II-C	9.0	8.0	6.6	2
RXJ1514.0–4629B	11.17	K7	0.479	0.349	−0.24	II-C	8.0	14.0	7.5	2
RXJ1514.2–4103	9.64	G7	0.174	−0.050	3.82	Ia	26.1	26.5	7.3	1
RXJ1514.7–3445	9.02	F5	0.150		4.12	Ia		115.0	3.1	2
RXJ1515.8–3331	9.69	K0	0.358	0.050	1.57	Ia	25.0	24.0	0.6	2
RXJ1515.9–4418	11.33	K1	0.471	0.137	−1.03	II-C	18.0	16.0	7.0	2
RXJ1516.6–4406	10.73	K2	0.566		0.00	If	121.2	135.0	−2.6	1
RXJ1517.8–3706A	12.75	M1.5	0.527	0.388	−3.93	I	9.0	8.0	4.5	2
RXJ1517.8–3706B	11.80	K7-M0	0.220	0.090	−1.35	II-C	33.0		6.4	2
RXJ1518.5–3738	9.91	K1	0.347	0.013	0.00	If	25.0	23.0	3.4	2
RXJ1518.9–4050	9.97	G8	0.477		1.37	Ia	178.4	230.0	−3.1	1
RXJ1519.3–4056	10.24	K0	0.408	0.100	−0.28	II-C	17.3	18.0	5.7	1
RXJ1522.2–3959	10.73	K3	0.495	0.136	−1.80	III-B	49.0	45.0	13.3	2
RXJ1523.4–4055	10.71	K2	0.391	0.048	0.00	If	9.9	12.0	6.8	1
RXJ1523.5–3821	11.77	M2	0.378		−5.93	Im	54.9	50.0	−12.8	1
							26.9		23.8	
RXJ1524.0–3209	10.65	K7	0.365	0.235	−2.26	I	12.2	13.0	22.7	1
RXJ1524.5–3652	10.29	K1	0.351	0.017	−0.07	II-C	19.0	17.5	4.2	2
RXJ1525.3–3845	7.99	G5	0.157	−0.054	3.29	Ia	16.0		1.9	2
RXJ1525.5–3613	10.38	K2	0.427	0.084	−0.29	I	61.9	56.0	4.8	1
RXJ1525.6–3537	10.85	K6	0.464		−1.56	Im	29.8		−7.5	1
							22.3		26.1	
RXJ1526.0–4501	10.00	G5	0.308	0.097	2.40	Ia	26.4	24.0	5.8	1
RXJ1534.1–3916	9.84	K1	0.241	−0.093	0.00	If	43.0	38.0	−14.8	2
RXJ1538.0–3807	11.03	K5	0.460	0.122	−0.82	II-C	18.0	14.0	3.4	2
RXJ1538.6–3916	10.34	K4	0.378	0.026	0.12	Ia	7.0	8.0	3.1	2
RXJ1538.7–4411	9.58	G5	0.351	0.140	0.00	If	21.0		4.1	2
RXJ1540.7–3756	10.93	K6	0.485	0.229	−0.49	II-C	19.6	18.0	3.9	1
RXJ1543.1–3920	10.83	K6	0.435	0.179	−0.13	II-C	14.0	9.0	4.7	2
RXJ1546.7–3618	10.21	K1	0.381	0.047	−0.57	II-C	7.1	12.0	2.5	1
RXJ1547.7–4018	10.03	K1	0.385	0.051	0.63	Ia	10.0	11.0	2.8	2
RXJ1550.0–3629	10.41	K2	0.373	0.030	−0.06	II-C	9.7	12.0	4.4	1
RXJ1552.3–3819 ^p	11.55	K7	0.460	0.330	−0.70	II-C	15.3	14.0	4.9	1
RXJ1554.9–3827 ^p	11.57	K7	0.545	0.415	−1.94	I	27.5	22.5	2.2	2
RXJ1555.4–3338	11.05	K5	0.462	0.124	−1.20	II-C	13.6	12.0	2.6	1
							11.0	8.0	0.7	2
RXJ1555.6–3709 ^p	11.04	K6	0.501	0.245	−0.61	II-C	18.0	11.0	2.0	2
RXJ1556.1–3655	11.86	M1	0.470	0.333	−82.60	II-R	13.8	13.0	0.0	1
RXJ1559.0–3646	11.38	M1.5	0.416	0.277	−3.05	II-C	19.0	15.0	1.0	2
RXJ1559.3–3814 ^p	11.47	M1.5	0.180		−1.24	II-C	7.0	10.0	−14.4	2
			0.225				6.0	10.0	18.8	
RXJ1559.8–3628	9.66	K3	0.476	0.117	−0.45	II-C	16.0	14.0	0.1	2
RXJ1601.2–3320	9.81	G8	0.308	0.077	1.92	Ia	21.9	21.0	3.0	1
RXJ1602.0–3613	10.57	K3	0.435	0.076	−0.85	II-C	30.4	28.0	−39.5	1
RXJ1603.2–3239	11.25	K7	0.574	0.444	−2.45	II-C	15.0	14.0	−0.9	2
RXJ1603.8–4355	8.65	K1	0.580	0.246	0.00	If		62.0	−1.0	2
RXJ1603.9–3938 ^p	9.79	K3	0.245		−0.03	III-B	8.0		−21.3	2
			0.164				8.0		27.8	
RXJ1604.5–3207	9.84	K2	0.354	0.011	−0.19	II-C	28.0	27.0	0.3	2
RXJ1605.0–3857 ^p	8.62	G2	0.166	−0.023	3.93	Ia	35.0		1.0	2
RXJ1605.6–3837 ^p	12.19	M1	0.298	0.161	−2.63	II-C	12.0	12.0	2.0	2
RXJ1607.2–3839 ^p	10.95	K7	0.568	0.438	−2.39	I	30.0	29.0	6.7	2
RXJ1608.3–3843 ^p	10.60	K7	0.495	0.365	−1.04	II-C	20.0	15.0	1.3	2
RXJ1608.5–3847 ^p	11.28	M2	0.649	0.508	−6.17	III-R	21.4	20.0	−2.5	1
RXJ1608.6–3922 ^p	11.45	K6	0.482	0.226	−14.20	II-C	21.8	20.0	1.2	1
RXJ1608.9–3905 ^p	9.74	K2	0.491	0.148	−0.09	I		49.0	−0.6	2
RXJ1609.7–3854 ^p	10.00	K5	0.597	0.259	−0.39	II-C	35.4	33.0	−3.7	1
RXJ1610.1–4016 ^p	10.11	K2	0.420	0.077	−0.27	I	57.7	54.0	5.1	1
RXJ1613.0–4004 ^p	11.36	K7	0.540	0.410	−0.41	III-B	60.3	55.0	−2.8	1

Table 1 – continued

Designation	I_C [mag]	SpT	W_{Li} [Å]	ΔW_{Li} [Å]	$W_{H\alpha}$ [Å]	$P_{H\alpha}$	$V \sin i_{CC}$ [km s ⁻¹]	$V \sin i_{FFT}$ [km s ⁻¹]	V_{RAD} [km s ⁻¹]	OB
RXJ1615.3–3255	10.50	K5	0.558	0.220	–18.90	II-C	17.0	13.0	–2.4	2
RXJ1623.5–3958	10.03	G3	0.241	0.043	2.53	Ia		33.0	4.7	2
Sz 77	10.83	M0	0.546		–17.10	III-R	12.0	9.0	–1.4	2
Sz 82	10.20	M0	0.604		–3.90	III-R	18.0	16.0	–1.0	2
Sz 96	11.84	M1.5	0.617		–6.10	IV-R	11.0	10.5	–5.1	2
Sz 129	11.09	K7-M0	0.453		–43.90	III-R	9.0	8.0	–0.7	2

velocities – which can provide further clues on membership of the Lupus SFR – as well as projected rotational velocities $V \sin i$. In addition, they provide much better estimates of the Li I equivalent widths than the medium-resolution spectra presented by Krautter et al. (1997). In this paper, we will mainly discuss the implications of our observations for the question of the pre-main-sequence nature of the *ROSAT* WTTSs in Lupus, as well as for the structure of the Gould Belt towards this direction. A more detailed study of Lithium abundances, surface gravities etc. will be the subject of another paper (Hauschildt et al., in preparation).

2 OBSERVATIONS AND DATA REDUCTION

Data for this project were obtained during two observing runs. Observations were performed for three nights at the ESO 3.6-m telescope with CASPEC (April 13 to 15, 1995), and for four more nights at the CTIO 4-m telescope with the cassegrain echelle spectrograph (April 26 to 29, 1997).

CASPEC was used in the short camera configuration with the red cross-disperser and a 31.6 gr mm⁻¹ echelle grating. The detector was a Tektronix TK512 CCD with 512² pixels and a pixel size of 27 μm (ESO no. 32). A slit width of 2.1 arcsec was used, yielding a nominal resolving power $\lambda/\Delta\lambda$ of 20 000. The spectra covered the range from 580 to 850 nm.

At the CTIO 4-m telescope, the echelle spectrograph was used with the Red Long camera, a 31.6 gr mm⁻¹ echelle grating and the G181 cross disperser. The detector was a Tektronix 2048 × 2048 CCD, used in double-readout mode. The slit width was set to 1.2 arcsec, and the resulting resolution was $\lambda/\Delta\lambda = 34 000$. The spectra covered the range from 480 to 720 nm.

Target stars were selected from the list of *ROSAT* WTTSs given by Krautter et al. (1997). This sample comprises both stars found by a raster scan of pointed *ROSAT* observations in regions of high visual extinction (the ‘on-cloud’ sample), and stars found by the RASS in less obscured regions (the ‘off-cloud’ sample). As shown by Wichmann et al. (1997a), ‘on-cloud’ is on average younger. No preference was given to particularly ‘promising’ objects, that is stars with large Li I equivalent widths, but, rather, targets were chosen to cover a large range in spectral type and age (as listed in Wichmann et al. 1997a). Note that this is not equivalent to a random selection, as large subsamples confined to small regions in the HR diagram will be underrepresented by such a uniform sampling. This is especially the case for stars discovered from the deep pointed observations in visually obscured regions of the Lupus SFR; these stars are typically very young (if at the distance of the Lupus SFR), faint, low-mass M-type stars.

A total of 62 stars could be observed during these runs – 27 during the first run, and 36 during the second run (one star, RX J1555.4–3338, was observed in both runs). 15 of these 62 stars belong to the ‘on-cloud’ sample. In addition, during the second

run four bona-fide Lupus TTS (Sz 77, 82, 96, and 129) from the list of Krautter (1991) were observed, in order to augment the literature data on the radial velocities of Lupus TTS (Dubath, Reipurth & Mayor 1996). The signal-to-noise ratio of our spectra ranges from 50 to about 100.

All data were reduced using IRAF. First, the bias was subtracted and the two-dimensional spectra were flat-fielded. Owing to the double-readout mode used for the CTIO data, the CCD area consisted of two parts with different gains and biases. Bias subtraction and flat-fielding was done separately for each of the two halves.

The individual echelle orders were extracted and wavelength-calibrated using standard tasks from the IRAF echelle reduction package. The orders were normalized by fitting low-order cubic splines both along and across the dispersion direction (the latter helped in removing the effect of strong lines within an order on the fit along the dispersion), and merged to form a single spectrum for each star.

3 RESULTS

3.1 Lithium equivalent widths

One of the prime goals of this study was to ascertain the classification of the target objects as PMS stars. While Li is known to be depleted during the PMS phase, it is also known that, depending on their spectral type, i.e. effective temperature, ZAMS stars still can show substantial Li equivalent widths. It has been pointed out (Briceño et al. 1997) that on the basis of medium-resolution spectra – as used by Wichmann et al. (1996), Krautter et al. (1997), and Alcalá et al. (1995, 1996) – the equivalent width of the Li I $\lambda 6708$ absorption line could be severely overestimated, leading to many erroneous detections of ‘PMS’ objects.

The equivalent widths (W_{Li}) of the Li I $\lambda 6708$ line, as listed in Table 1, were measured using both direct integration and a Gaussian fit, and the results of the two methods are in good agreement. The typical error of W_{Li} is about 20 mÅ, and is mainly due to uncertainty in the location of the continuum. In discussing these data, we first want to draw attention to the fact that there is *not a single star* in the sample in which Li is not clearly detected in absorption. This rules out the theory that the Li feature seen in medium-resolution spectra is just due to a blend of other lines, and that a large fraction of the *ROSAT* WTTSs are misclassified old main-sequence stars.

From Fig. 1 it can be seen that the stars selected for this study represent a fair subsample of the Krautter et al. (1997) sample with respect to W_{Li} . However, of the 15 stars with $W_{Li} \leq 0.25$ Å only four were observed. Out of these 15 ‘low-Li’ stars, four are early-type (G) stars, while all the others are M-type stars, mostly (nine) located in regions of high visual extinction and discovered by deep pointed observations. Two of the early-type ‘low-Li’ stars were observed and found to be ZAMS stars. Also, two ‘low-Li’

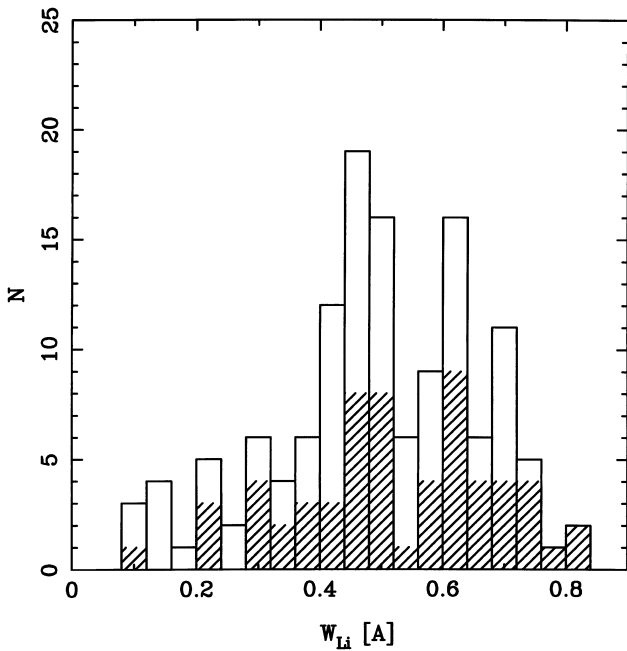


Figure 1. Histogram of (raw) W_{Li} for the Lupus WTTs discovered by Krautter et al. (1997), as measured on their spectra (solid lines), and the subsample selected for this study (hatched area).

M-type stars were observed, and both were confirmed as PMS. Given their location within regions of high extinction, and the higher reliability of low-resolution Li detection for M-type stars (see below), we think that most of these ‘low-Li’ M-type stars might be PMS.

Using the Pleiades as a reference for ZAMS stars, we define $\Delta W_{\text{Li}} = W_{\text{Li}} - \text{Max}(W_{\text{Li}, T_{\text{eff}}})_{\text{Pleiades}}$ as the excess in Li absorption W_{Li} with respect to the maximum observed Li equivalent width in Pleiades stars at the same effective temperature $\text{Max}(W_{\text{Li}, T_{\text{eff}}})_{\text{Pleiades}}$; that is, a positive value of ΔW_{Li} indicates that the star is located above the Pleiades upper envelope in a $T_{\text{eff}}-W_{\text{Li}}$ diagram. Fig. 2 shows the location of the *ROSAT* WTTs (this work) in such a $T_{\text{eff}}-W_{\text{Li}}$ diagram, along with ZAMS Pleiades stars (Soderblom et al. 1993), and optically discovered bona fide TTSs (Basri, Martin & Bertout 1991; Magazzù, Rebolo & Pavlenko 1992; Martin et al. 1994). Soderblom et al. (1993) give equivalent widths corrected for the contribution of the Fe I $\lambda 6707.44$ line. For consistency, all other data points in the plot have been corrected for this line as prescribed by Favata et al. (1993). T_{eff} for the *ROSAT* WTTs is from Wichmann et al. (1997a).

We have discarded the X-ray-discovered stars from the Martin et al. (1994) sample to avoid biasing the bona fide TTS sample. We have also discarded four binaries and four ultrafast rotators (UFRs) from our *ROSAT* WTTs sample, as both present difficulties for the determination of W_{Li} – in UFRs the line is blended, while in binaries the continuum, relative to which the equivalent width is measured, is the sum of two continua, thus invalidating the equivalent width. Excluding these stars, we have a total of 54 *ROSAT* WTTs in Lupus with high-resolution spectra available.

We can see that nearly all of them are located above the Pleiades upper envelope. Only five out of these 54 *ROSAT* WTTs are located below the Pleiades upper envelope, putting their PMS nature in doubt. If we adopt the more conservative criterion of

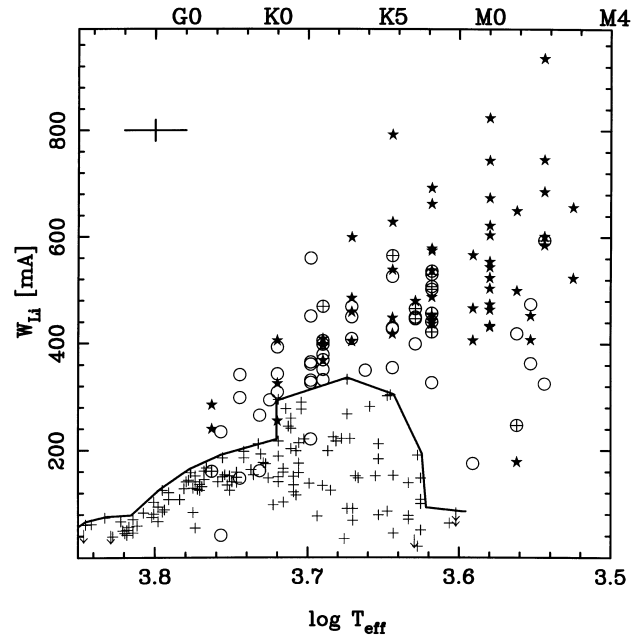


Figure 2. W_{Li} versus T_{eff} for Pleiades (crosses), *ROSAT*-discovered Lupus WTTs (open circles), and optically discovered bona fide TTSs (stars). Also drawn is the upper envelope for the Pleiades sample. TTS and *ROSAT* WTTs data have been corrected as described in the text. Typical error bars are shown upper left. On the upper border spectral types are indicated. *ROSAT* WTTs from pointed observations are marked by encircled crosses.

Covino et al. (1997), requiring $\Delta W_{\text{Li}} \geq 20 \text{ mÅ}$ for a PMS star (to account for measurement errors), only four more stars have to be regarded as doubtful PMS candidates. Note, however, that the bona fide TTS RY Tau is located slightly below the Pleiades upper envelope. There is apparently significant spread in W_{Li} for each given effective temperature T_{eff} , which might be due to stellar rotation (Soderblom et al. 1993). Thus, for stars near the borderline, a PMS nature cannot be excluded. This result shows that medium-resolution spectra with a resolution of about 4 Å , as used in the RASS papers, can be a robust tool to single out stars with high W_{Li} . A large majority of the new WTTs discovered in Lupus (Krautter et al. 1997) show a W_{Li} clearly in excess of ZAMS star values, and have to be regarded as bona fide PMS stars.

In Fig. 3 we plot $f(W_{\text{Li}}) = W_{\text{Li},h}/W_{\text{Li},m}$ versus T_{eff} , where $W_{\text{Li},h}$ denotes the equivalent width measured from our echelle spectra, and $W_{\text{Li},m}$ denotes the value measured on the medium-resolution spectra of Krautter et al. (1997). Apparently, at a resolution of about 4 Å as used in the study of Krautter et al. (1997), W_{Li} is overestimated by about 20 per cent in the mean. The effect seems to depend on temperature, with overestimation of W_{Li} almost negligible for M stars, but increasing towards higher temperature. This result is in good agreement with that of Covino et al. (1997). However, as shown above, in spite of this overestimation we find that the vast majority of the *ROSAT* WTTs in Lupus are indeed PMS stars.

The spatial distribution of observed and unobserved stars of the Krautter et al. (1997) sample is shown in Fig. 4.

3.2 The $H\alpha$ line

As opposed to classical T Tauri stars (CTTSs), WTTs typically do not display evidence for ongoing accretion of circumstellar

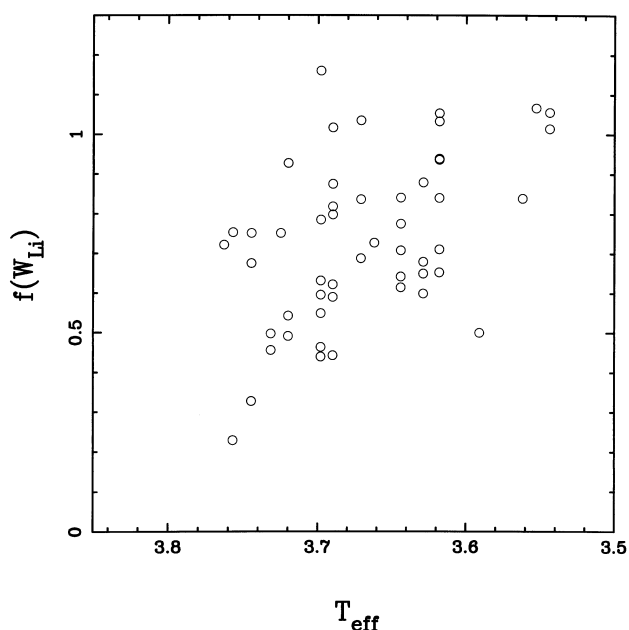


Figure 3. $f(W_{\text{Li}})$ versus T_{eff} for new Lupus WTTSs studied in this work. $f(W_{\text{Li}})$ is defined as the ratio of $W(\text{Li}, \text{high resolution})$ to $W(\text{Li}, \text{medium resolution})$.

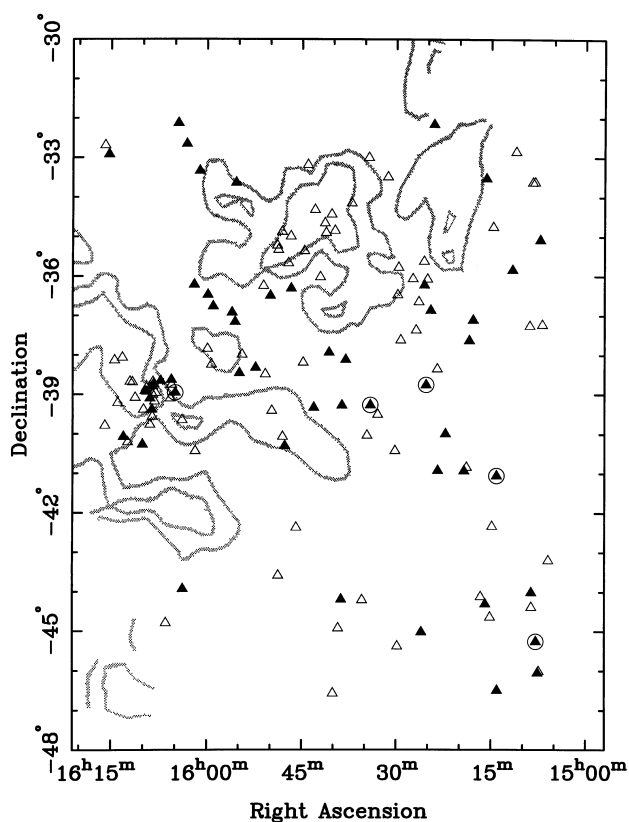


Figure 4. Spatial distribution of observed (filled triangles) and unobserved stars from the Krautter et al. (1997) sample. CO contours are from Murphy et al. (1986) (only part of the region is covered by their survey). Stars classified as ZAMS are circled.

matter, and the average age of the *ROSAT* WTTSs is found to be significantly in excess of that of the CTTS in Lupus (Wichmann et al. 1997a). Moreover, from Fig. 2 it can be concluded that the *ROSAT* WTTSs represent an intermediate stage of evolution between the optically discovered TTSS found in dark clouds, and ZAMS stars.

One of the typical features of classical T Tauri stars is their strong and broad $H\alpha$ emission lines, with equivalent widths $W_{H\alpha}$ up to more than 100 \AA , and wings extending to velocities of several 100 km s^{-1} . Models to explain these features by chromospheric emission have failed, and it is commonly accepted that the Balmer emission lines arise either in a wind (cf. Mitskevich, Natta & Grinin 1993) or in magnetic accretion columns (Calvet & Hartmann 1992; Hartmann, Hewett & Calvet 1994).

On the other hand, the situation is very different for young active late-type main-sequence stars that display a variety of $H\alpha$ line profiles ranging from pure absorption to weak emission (with $W_{H\alpha}$ typically below 5 \AA). In the latter case, the line often shows a central self-reversal, thus leading to a symmetric double-peaked profile (Panagi, Byrne & Houdebine 1991). Contrary to the case for CTTSs, the line emission in these stars can be modelled quite successfully by purely chromospheric emission (cf. Houdebine & Stempels 1997).

Reipurth, Pedrosa & Lago (1996) have presented a scheme for the classification of T Tauri $H\alpha$ line profiles by subdividing them into the following four classes: (I) single peak; (II-R/B) double peak with red or blue absorption trough; (III-R/B) like (II), but the height of the secondary peak is less than the half-height of primary peak; and (IV-R/B) P-Cygni/inverse P-Cygni profile. To account for line profiles found in active main-sequence stars, we have added the following classes: (Ia) absorption, (If) filled-in, and (II-C) central absorption. The results are presented in Table 1, along with $W_{H\alpha}$.

We have measured $W_{H\alpha}$ using direct integration (without prior subtraction of a template spectrum). As for W_{Li} , the error is about 20 m\AA , mainly due to uncertainty of the continuum. For the majority of the *ROSAT* WTTSs in our study, both $W_{H\alpha}$ and the range of observed line profiles agree with the typical features of active main-sequence stars (comprising line profiles Ia, If, I, and II-C, but excluding II-B/R, III and IV). Therefore we believe that in these stars the $H\alpha$ line emission is most likely chromospheric in origin; that is, the observed activity in these stars represents an extreme level of the activity of late-type main-sequence stars, rather than a low level of CTTS-like (accretion-driven) activity. [We refrain from a more detailed comparison of $W_{H\alpha}$ with values measured for ZAMS stars, for example by Soderblom et al. (1993), as these are measured in a different way – by subtracting a template spectrum – and thus are not directly comparable.]

We note in passing that the $H\alpha$ line profiles of the CTTSs Sz 77 and 82 apparently have changed since observed by Reipurth et al. (1996). Both are of type III-R now, while Reipurth et al. (1996) report type I for Sz 77 and type IV-R for Sz 82. Thus in Sz 77 a red absorption has developed, while in Sz 82 the inverse P-Cygni absorption has disappeared. Such changes are rather common in CTTSs; see for example Krautter & Bastian (1980).

3.3 Radial velocities

Radial velocities V_{rad} were obtained by cross-correlating our spectra with a numerical mask that was constructed from a spectrum of an F-type star. A more detailed description of the method is given by Covino et al. (1997). (As discussed there, a K-type mask was

also tested, but the results were essentially identical.) Zero-points were established from observations of radial velocity standards each night during the observing runs. The results are listed in Table 1. Individual errors are about $\pm 1 \text{ km s}^{-1}$, and a zero-point error of the order of $\leq 0.5 \text{ km s}^{-1}$ may be present (see next paragraph).

As in our two runs different instruments and set-ups were used, a systematic difference between the data sets might have arisen. Thus, we compared the data obtained at CTIO and ESO in order to check for such an effect. In Fig. 5 we show the distributions of V_{rad} separately for both samples. Obviously both samples contain some outliers, located in opposite directions, that will bias their means in opposite ways. However, if we eliminate these outliers by cutting both samples at $\pm 3\sigma$ (i.e. $-12 \text{ km s}^{-1} \leq V_{\text{rad}} \leq 18 \text{ km s}^{-1}$), we obtain mean radial velocities of 3.0 ± 0.9 and $2.7 \pm 0.5 \text{ km s}^{-1}$ for the ESO and the CTIO samples, respectively. Thus we conclude that there is no evidence for any systematic difference between the ESO and CTIO samples, although we cannot rule out a zero-point difference of the order of $\leq 0.5 \text{ km s}^{-1}$.

In Fig. 6 we compare our data on *ROSAT* WTTs in Lupus with data on bona fide Lupus CTTs. The latter group comprises nine stars, five from Dubath, Reipurth & Mayor (1996) and four from our own observations. The mean radial velocity of these nine Lupus CTTs is $\bar{V}_{\text{rad}} = -0.03 \pm 1.2 \text{ km s}^{-1}$, in good agreement with the radial velocity of the Lupus clouds from CO observations [for the CO, Dame et al. (1987) give a velocity of $+5 \text{ km s}^{-1}$ with respect to the local standard of rest (LSR), which converts to a heliocentric velocity of 0 km s^{-1}].

On the other hand, for the 49 *ROSAT* WTTs in Lupus with $\Delta W_{\text{Li}} > 0$, we obtain a mean radial velocity $\bar{V}_{\text{rad}} = +2.72 \pm 1.15 \text{ km s}^{-1}$ (i.e. $\bar{V}_{\text{LSR}} = +7.7$). Split into the ‘on-cloud’ and the ‘off-cloud’ samples (see Fig. 6), the respective radial velocities are $+1.29 \pm 0.87 \text{ km s}^{-1}$ and $+3.17 \pm 1.39 \text{ km s}^{-1}$. There is no statistical significant difference between the Lupus CTTs and our ‘on-cloud’ sample, while the difference between CTTs and ‘off-cloud’ sample is highly significant at the 0.4 per cent level (i.e. the probability of both having equal means is 0.4 per cent). The difference between ‘on-cloud’ and ‘off-cloud’ is also significant at the 3 per cent level (for evaluation, the non-parametric Wilcoxon and logrank tests were used).

We would like to point out that with pure differential galactic rotation, positive values of V_{LSR} are ‘forbidden’ in the fourth galactic quadrant. Positive values of V_{LSR} are, however, observed for the youngest disc stars because of the expansion of the Gould Belt system. The radial velocities of the *ROSAT* WTTs provide evidence that they belong to this system, just like the Lupus dark clouds, thus strengthening earlier results by Wichmann et al. (1997b).

With respect to the small difference in velocities between *ROSAT* (‘off-cloud’) WTTs in Lupus and Lupus CTTs, we note that the expanding gas pertaining to the Gould Belt system decelerates due to the pressure of the ambient interstellar gas into which it is expanding. This deceleration will depend strongly on the local density of the ambient gas. As the *ROSAT* WTTs in Lupus are somewhat older than the Lupus CTTs, conditions might have changed since their formation, and thus a difference in velocities would not be unexpected.

Note also that there are several stars with $\Delta W_{\text{Li}} < 0$ that do not show deviant radial velocities, indicating that they also might be Gould Belt stars, although probably of somewhat higher age.

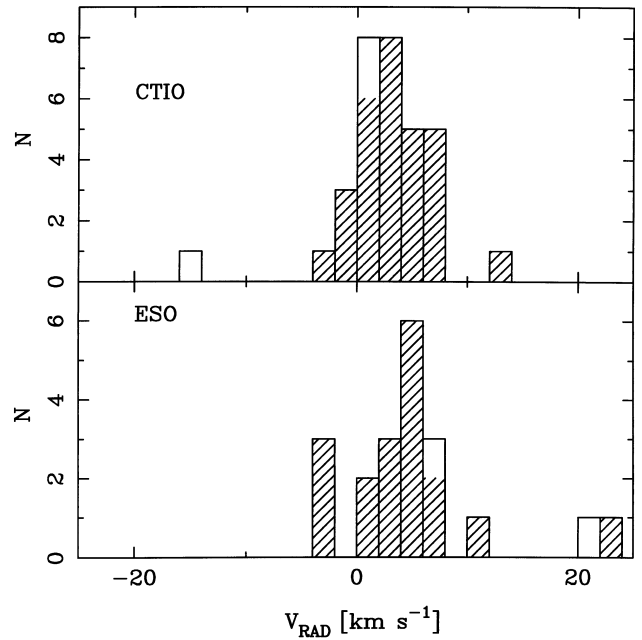


Figure 5. Distribution of radial velocities for stars observed at CTIO (upper panel) and ESO (lower panel). Filled areas represent stars with $\Delta W_{\text{Li}} > 0$.

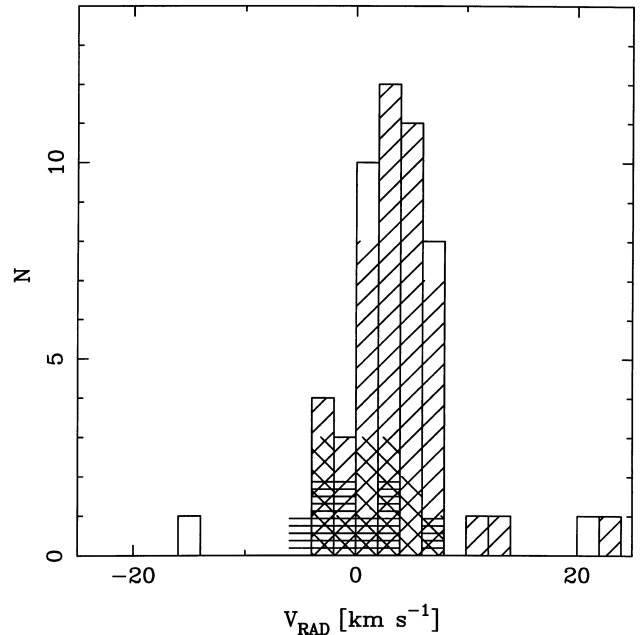


Figure 6. Distribution of radial velocities for Lupus CTTs (hatched horizontally) and *ROSAT* WTTs in Lupus. Diagonally hatched areas represent *ROSAT* WTTs with $\Delta W_{\text{Li}} > 0$. The subset of ‘on-cloud’ *ROSAT* WTTs is diagonally cross-hatched.

3.4 Projected rotational velocities

Projected rotational velocities $V \sin i$ were obtained by two different methods, namely cross-correlation and FFT (fast Fourier transformation). Details of these methods can be found in Covino et al. (1997). As discussed there, cross-correlation probably is the superior method for slow rotators, while for fast rotators FFT will give better results, mainly because the shape of the

cross-correlation function becomes strongly non-Gaussian for fast rotators, and its width cannot easily be defined anymore.

Results for both methods are given in Table 1. Within the errors (ranging from about 2 km s^{-1} for $V \sin i < 20 \text{ km s}^{-1}$ to 5 km s^{-1} for $V \sin i > 50 \text{ km s}^{-1}$), both methods agree very well. Consistent with Covino et al. (1997), we will use results from cross-correlation for $V \sin i \leq 15 \text{ km s}^{-1}$, and results from FFT for faster rotators.

It is known that there is a tight correlation between stellar rotation and X-ray activity (Wichmann et al. 1998a; Bouvier 1990). Thus the distribution of $V \sin i$ as obtained in this work presumably is biased against slow rotators. In Fig. 7, we show this distribution, along with the distributions of (i) a sample of optically selected T Tauri stars (compiled from Bouvier et al. 1986; Bouvier 1990; Hartmann, Soderblom & Stauffer 1987; and Hartmann & Stauffer 1989); and (ii) Pleiades ZAMS stars (compiled from Jones, Fischer & Stauffer 1996; Soderblom et al. 1993; Stauffer & Hartmann 1987; and Stauffer et al. 1984). To account for the mass dependence of PMS evolution and the very low number of optically selected TTSs with measured $V \sin i$ at high masses, we have restricted the plot to masses between 0.7 and 0.9 solar masses (masses for WTTs are taken from Wichmann et al. 1997a).

Contrary to optically selected TTSs, the *ROSAT* WTTs typically do not show evidence for disc accretion any more. On the other hand, their W_{Li} is higher than that observed for Pleiades stars. Thus the *ROSAT* WTTs represent an evolutionary state between the two, and we might expect them also to have an intermediate distribution of $V \sin i$.

Fig. 7 shows that the ratio of stars with $0 \leq V \sin i < 10 \text{ km s}^{-1}$ to stars with $10 \leq V \sin i < 20 \text{ km s}^{-1}$ is smaller for the optically selected TTSs than for the Pleiades.

However, for the *ROSAT* WTTs the ratio of stars with $0 \leq V \sin i < 10 \text{ km s}^{-1}$ to stars with $10 \leq V \sin i < 20 \text{ km s}^{-1}$ is lower than for both other samples; that is, we observe a lack of slow rotators for the stars in our sample. This can be explained by

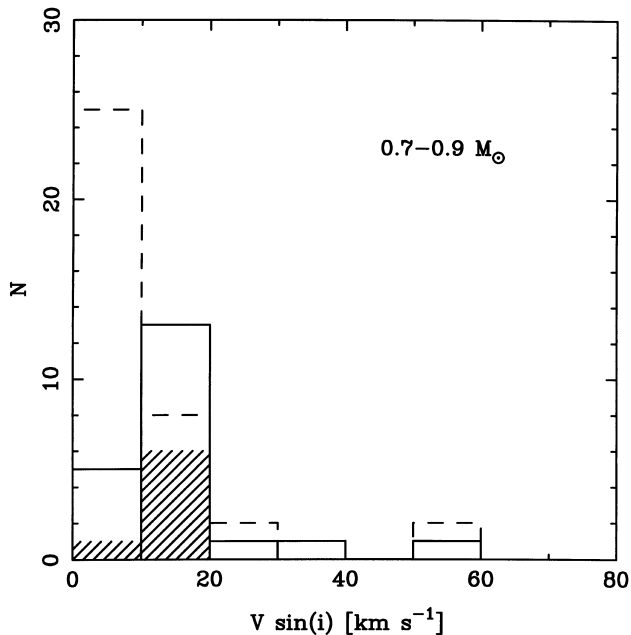


Figure 7. Distribution of projected rotational velocities for optically detected TTSs (solid lines), Pleiades ZAMS stars (dashed lines), and *ROSAT* WTTs (only ‘off-cloud’ sample) with $\Delta W_{\text{Li}} > 0$ (hatched area).

an observational bias due to the X-ray selection of the *ROSAT* WTTs, demonstrating once again the connection between stellar activity and rotation.

The distance of the *ROSAT* WTTs has been a controversial issue. If these stars were ZAMS stars, as Briceno et al. (1997) argue, they should be significantly less distant than the SFRs to which they have been attributed in the RASS papers, in order to be located on the ZAMS. We will show now that, at least for the mean distance of the Li-rich stars in Lupus, this is not the case.

If the rotational period P_{rot} as well as $V \sin i$ and $\sin i$ are known, then the stellar radius R can be computed straightforwardly as

$$R = \frac{P_{\text{rot}} V \sin i}{2\pi \sin i}.$$

The distance r of the star then might be estimated as

$$r = \sqrt{\frac{R^2 \pi B_{\nu, T_{\text{eff}}}}{C_{\nu, T_{\text{eff}}} f_{\nu}}},$$

where $B_{\nu, T_{\text{eff}}}$ denotes the flux of a blackbody of temperature T_{eff} at the frequency ν , f_{ν} the observed flux from the star, and T_{eff} the effective temperature of the star (as inferred from the spectral type). $C_{\nu, T_{\text{eff}}}$ is a correction factor of order unity obtained from model spectra (Hauschildt, Allard & Baron 1999), to account for deviation of the stellar flux from the blackbody law.

For a large number of stars in our sample, P_{rot} has been measured by Wichmann et al. (1998a), while I_C magnitudes and extinction values are given by Wichmann et al. (1997a). The inclination angle for *individual* stars is of course not known, and therefore it is not possible to compute the radii and distances of individual stars. However, we can set $\sin i$ to its mean value of $\pi/4$ (for an isotropic distribution of inclination angles), and average over the whole sample to obtain a mean value of the distance. The resulting distance is $r = 154 \text{ pc}$ (for stars with $\Delta W_{\text{Li}} > 0$).

We evaluated the error by a Monte Carlo simulation. While $\sin i$ may be wrong by a factor of 2 for any individual star (see the discussion on bias below for limits on $\sin i$), other observables in the equations above have typical errors of a few per cent. We therefore regard the unknown inclination as the main source of error. We assigned to the stars of our sample random values of $\sin i$, P_{rot} , and $V \sin i$. A random normal distribution was chosen for the distances, and f_{ν} was computed to be consistent with the random parameters. Then the mean distance of the simulated sample was estimated by the equations given above.

Repeating this experiment 1000 times, we found that the difference Δ_r between estimated and true mean distances has a mean value of zero and a standard deviation of 6 per cent. We varied the mean distance assigned to the stars between 100 and 250 pc, and also the width of its distribution between 20 and 60 pc, but found no significant change in the standard deviation of Δ_r . In fact we found the standard deviation of Δ_r rather insensitive to the actual shape of the distance distribution of the parent population, as it remains the same even for a uniform distribution of distances.

However, another possible source of error is that the detection of photometric periods could be biased towards stars with high inclination angle, thus invalidating our assumption of an isotropic distribution of the inclination angle (obviously, at an inclination angle of zero a spot would never produce any brightness variation). Wichmann et al. (1997a) report period detections for 34 out of 46 stars studied by them (i.e. 74 per cent). There might be several reasons for non-detections (e.g. absence of a

sufficiently large spot), but as the most conservative estimate, we may attribute all non-detections to a too low inclination angle.

This would give a lower limit of 42° for the inclination angle (as derived from numerically integrating the probability density function of the inclination angle, which is proportional to $\sin i$). We have repeated our simulations with the inclination angle limited to values between 42° and 90° , and we find that in this case, using $\pi/4$ (i.e. the mean for an isotropic distribution) for $\sin i$ would overestimate the distance by 13 per cent. We thus conclude that the mean distance to those *ROSAT* WTTs with $\Delta W_{\text{Li}} > 0$ in the direction of the Lupus SFR is in the range 135–165 pc. Within errors, this distance is still marginally consistent with the *Hipparcos* distance of the Lupus SFR, which has been estimated as 190 ± 27 pc (Wichmann et al. 1998b). Furthermore, it is perfectly consistent with the previous distance estimate of 140 ± 20 pc by Hughes, Hartigan & Clampitt (1993), which was adopted by Wichmann et al. (1997a) to place the stars in the HR diagram.

Fig. 8 shows a histogram of the distribution of distances. Distributions for the ‘off-cloud’ and the ‘on-cloud’ samples are plotted separately, but there is no significant difference. The histogram is suggestive of a peaked distribution, with a tail towards lower distances. While this is what we would expect for a young Gould Belt population, given the possible bias for period detections the actual distribution of $\sin i$ is uncertain, and thus we would not put too much weight on this result.

Using *Hipparcos* parallaxes, Neuhäuser & Brandner (1998) found that four out of six *ROSAT* WTTs in Lupus observed by *Hipparcos* had parallaxes consistent with the distance of the Lupus SFR. The other two (RX J1504.8–3950 and CoD–36°10569) may be foreground stars. Neuhäuser & Brandner (1998) could place CoD–36°10569 in the HR diagram and showed that, although located at only about half the distance of the Lupus SFR, it still is a PMS star with an age of about 1.5×10^7 yr. We have no data on RX J1504.8–3950, but CoD–36°10569 has $\Delta W_{\text{Li}} = 116$ mÅ, confirming its PMS nature.

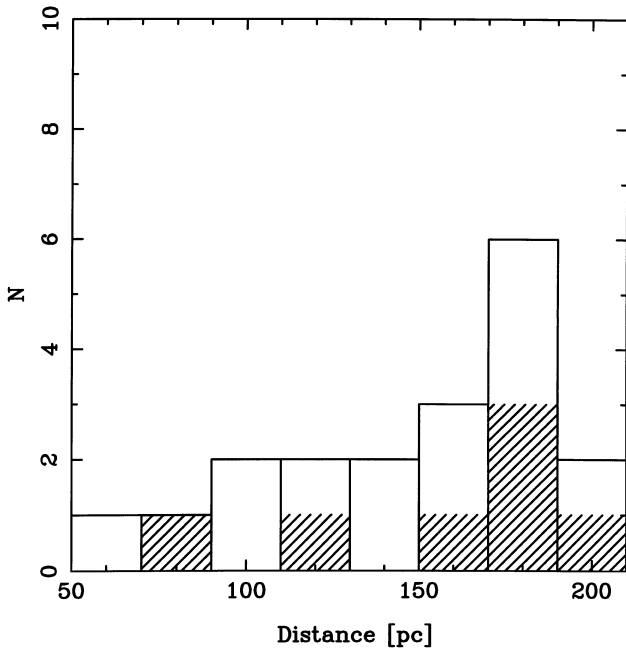


Figure 8. Distribution of distances computed for mean value of $\pi/4$ for $\sin i$. The solid line is for the ‘off-cloud’ sample, and the shaded area is for the ‘on-cloud’ sample.

For a proper interpretation of the *Hipparcos* data, one has to keep in mind that the *Hipparcos* sample is biased towards the brightest stars among the *ROSAT* WTTs (most of the *ROSAT* WTTs are fainter than the limiting magnitude of *Hipparcos*, and the *Hipparcos* catalogue is not complete to the limiting magnitude of the instrument). The brightest *ROSAT* WTTs are likely to be the nearest, and thus the fact that the *Hipparcos* data *in spite of their magnitude bias* give distances consistent with that of the Lupus SFR for four out of six stars, is in good agreement with our result of a mean distance similar to that of the Lupus SFR.

4 DISCUSSION

With regard to the *ROSAT* WTTs located in the Lupus SFR and its surrounding area, it has been observationally established that

- (i) the large majority of them show Li equivalent widths in excess of those observed in the Pleiades, i.e. they are younger than the Pleiades (this work);
- (ii) their mean distance is – within errors – in agreement with that of the Lupus SFR, and their mean velocities indicate that they recede from us at a similar, or (with respect to the ‘off-cloud’ sample) slightly larger pace (this work); and
- (iii) their spatial distribution is centred on the Gould Belt, and the width of their spatial distribution is about 10° – 15° , consistent with the width of the Gould Belt (Wichmann et al. 1997b).

These observations firmly establish that the vast majority of these stars are bona fide PMS stars belonging to the Gould Belt star-forming complex.

Our data indicate that many of these stars formed not far from the Lupus SFR, which represents a presently very active region at the outer edge of the expanding plane of the Gould Belt. However, as stars have been forming in the Gould Belt for several 10^7 yr by now, we expect, and our data also suggest this, a tail of nearer foreground Gould Belt stars.

The interaction between the expanding Gould Belt and the ambient interstellar gas presumably causes a complex and constantly changing pattern of star formation along the outer rim of the Gould Belt. The Lupus dark clouds might be the remnant of a once much larger SFR, in which the *ROSAT* WTTs formed. However, it might also be that many of the *ROSAT* WTTs formed in molecular clouds that have now completely dispersed. In that context, it is interesting that Mizuno et al. (1998) found that about 70 per cent of the isolated *ROSAT* WTTs in Chamaeleon can be associated with small CO clouds found close to them.

If further measurements for the CTTs in Lupus confirm the difference in radial velocities with respect to the *ROSAT* WTTs, this would indicate that the gaseous part of the Gould Belt in this region – comprising the Lupus SFR – has experienced some deceleration since the formation of the *ROSAT* WTTs, possibly due to ram pressure from the ambient interstellar gas. Thus, improved data will give important insights into the velocity structure of the Gould Belt towards Lupus.

Wichmann et al. (1997a) derived a mean age of about 10^7 yr for the *ROSAT* WTTs in Lupus. As we have shown, the distance of 140 pc used by them is probably a lower limit of the true mean distance. Thus, on average the luminosities of these stars are probably even higher, and the stars younger than estimated by Wichmann et al. (1997a). This is a rather important result, as placement in the HR diagram is a more secure method of determining the evolutionary status of stars than Lithium depletion, which is still poorly understood.

Previous to these observations, several authors (Briceño et al. 1997; Micela et al. 1997) claimed that most of these stars would turn out to be foreground ZAMS stars with distances of about 100–120 pc and ages similar to that of the Pleiades. There is obviously some contradiction between these claims and our observations, and we will now briefly discuss the possible reasons.

Briceño et al. (1997) argue that with the sensitivity of the RASS and the assumption of a constant star-forming rate in the solar neighbourhood, a large fraction of the *ROSAT* WTTs will be foreground stars, pertaining to a presumed ubiquitous population of widely dispersed ZAMS stars with ages of the order of 10^8 yr. However, Briceño et al. (1997) have confused the *detection limit* of the RASS, i.e. the flux of the faintest sources, with its *completeness limit*, i.e. the limit for which all brighter sources are detected.

The completeness limit of 10^{-13} erg cm $^{-2}$ s $^{-1}$ (equivalent to a count rate of about 0.01 count s $^{-1}$), as adopted by them, in fact corresponds to the RASS detection limit in the SFRs studied in the RASS papers. However, due to the non-uniform sensitivity of the RASS the true completeness limit is only about 0.03 count s $^{-1}$ (R. Neuhäuser, private communication), i.e. three times higher. Thus, using the Briceño et al. (1997) model and the correct completeness limit presumably will result in a significantly lower number of foreground ZAMS stars in the RASS than predicted by these authors. We do not doubt that the stellar population predicted by Briceño et al. (1997) most likely exists, but apparently the RASS is not as sensitive to it as the authors have assumed. We think that this is a population distinct from the *ROSAT* WTTs, except for some minor contamination.

Moreover, Briceño et al. (1997) assume that the ‘background’ to their foreground ZAMS stars is just the average galactic background. If instead this ‘background’ contains large numbers of very active, X-ray-bright PMS stars, the fraction of foreground stars in the RASS source counts naturally will go down, while the total source counts will go up. In fact Guillot et al. (1998) demonstrated a large excess in stellar source counts in the plane of the Gould Belt.

While we find that the major fraction of *ROSAT* WTTs in Lupus comprises PMS stars, Micela et al. (1997), based on *Hipparcos* parallaxes, found that most of the Li-rich cool dwarfs in the EMSS turned out to be ZAMS stars. They argue that this result can be applied to the *ROSAT* WTTs as well, which obviously is in contradiction to our data. Most probably the reason is that the EMSS was constrained to high galactic latitudes, far from any SFR. Thus, the parent population for the EMSS sample presumably is quite different from the parent population of the *ROSAT* WTTs, which are located within 10° of active SFRs, and also within a huge-star-forming complex – the Gould Belt. It might well be that the parent population of the Li-rich cool dwarfs in the EMSS is exactly the dispersed ZAMS population postulated by Briceño et al. (1997).

Finally, Palla & Galli (1997) argue that molecular clouds will produce stars only near the end of their lifetime, resulting in a narrow peak in the age distribution of the stars formed by a cloud, and a correspondingly very low probability of finding older PMS stars nearby. This argument is based on the assumption that the lifetime τ_{MC} of molecular clouds is comparable to the time-scale τ_{AD} of ambipolar diffusion.

However, this conclusion is at variance with the observed paucity of inactive (non-star-forming) molecular clouds. With the time-scales adopted by Palla & Galli (1997), namely $\tau_{MC} = 10$ – 20 Myr and $\tau_{AD} = 10$ Myr, the ratio R of active to inactive clouds would be in the range 0–1, while the observed ratio is

about 2.5–4 (Feigelson 1996). In fact τ_{MC} is a rather uncertain quantity that might be as high as 50 Myr (Falgarone & Puget 1986), and, in order to match the observed value of R , a value of τ_{MC} near the upper rather than near the lower limit should be chosen. This would provide a comfortably long period of the order of 30 Myr for star formation to proceed in a slow, possibly self-regulated (Silk 1985) way.

Moreover, Palla & Galli (1997) consider a molecular cloud as an isolated object. But the Lupus SFR is by no means an isolated object, rather it is a presently very active part at the outer edge of a huge, expanding star-forming complex, namely the Gould Belt, which has continuously formed stars for most of its present lifetime of 5 – 6×10^7 yr (cf. Comerón, Torra & Gómez (1994)). Even with short cloud lifetimes, we might expect plenty of PMS stars especially towards the outer edge of this complex.

5 CONCLUSIONS

Given the geometry of the Gould Belt, among all SFRs studied in the RASS papers Lupus would obviously be the prime candidate for yielding a fairly ‘clean’ sample of very young stars. The reason is that the Sun is located about halfway between the centre and the edge of the Gould Belt, with Lupus at the ‘near’ side of the edge. Thus, when looking towards Lupus, we are looking away from the Gould Belt’s centre, towards its outermost – and therefore youngest – part. Therefore, even foreground Gould Belt stars towards this direction should be very young.

The situation is less favourable for Chamaeleon, which is located about 15° off the plane of the Gould Belt (putting its physical connection in doubt), and in fact a relatively large contamination of the *ROSAT* WTTs with older stars has been found there by Covino et al. (1997).

In the direction of Taurus, we are looking towards the centre of the Gould Belt, i.e. towards its oldest part, thus a larger contamination with older stars, as seen by high-resolution spectroscopy (Wichmann et al., in preparation) might be expected there as well.

The region south of Taurus, studied by Neuhäuser et al. (1997), Magazzù et al. (1997), and Frink et al. (1997) is far from molecular clouds and from the Gould Belt, thus few very young stars would be expected there, in line with the observations.

The association of the bona fide PMS stars, and presumably at least some of the ZAMS stars, among the RASS WTTs with the Gould Belt thus naturally explains the fact that, towards other SFRs, a larger fraction of older stars is found within the *ROSAT* WTTs than towards Lupus.

The Briceño et al. (1997) hypothesis, on the other hand, does not offer such a natural explanation. As the population postulated by them is (i) foreground towards all studied SFRs, (ii) older than the Gould Belt, and (iii) results from a large-scale smoothing process, there is no natural explanation for a ‘hole’ towards Lupus within this hypothesis.

We would like to point out the important fact that already from simple star counts within the RASS catalogue, independent of any follow-up observations, the predominance of the Gould Belt above the background population is clearly visible (Guillot et al. 1998). This fits perfectly into our model of the *ROSAT* WTTs as to a large extent representing the low-mass stars of the Gould Belt starburst, as discussed above. ZAMS stars within the *ROSAT* WTTs sample might represent older stars from the population introduced by Briceño et al. (1997), but might also represent older stars of the Gould Belt.

The ‘Gould Belt model’ favoured by our group has some

common ground with the Briceño et al. (1997) model, insofar as both models invoke – in addition to stars that are members of the SFRs studied – some other population of young stars to explain the result of *ROSAT* observations of nearby SFRs. However, the two models are distinct with respect to the type of the additional stellar population invoked by them. The stellar population on which the Briceño et al. (1997) model is based is completely unrelated to the studied SFRs, while the Gould Belt, on which our model is based, is naturally connected to many nearby SFRs, and significantly younger than the population invoked by Briceño et al. (1997).

Our ‘Gould Belt hypothesis’, discussed in this paper, has important consequences for the study of the solar neighbourhood. While in the Briceño et al. (1997) hypothesis the young stellar population in the solar vicinity would be ‘typical’ for our Galaxy, the observed predominance of stars from the Gould Belt starburst indicates that we are located in a somewhat untypical region of the Galaxy that is very rich in very young stars. Such stars should be abundant in the solar neighbourhood, and we thus expect that objects like AB Dor could pop up in larger numbers once suitable surveys are undertaken.

To conclude this discussion, we think that the discovery of the *ROSAT* WTTs and their identification as PMS members of the Gould Belt opens an exciting new window to the study of this intriguing, yet poorly understood galactic structure, which has played a key role in star formation in the solar neighbourhood during the past several tens of millions of years.

ACKNOWLEDGMENTS

This work is based on observations collected at the European Southern Observatory, La Silla, Chile (observing program 55.E-0738), and at the Cerro Tololo Interamerican Observatory, which is operated by the Association of Universities for Research in Astronomy, under contract with the National Science Foundation.

This research has made use of the SIMBAD data base, operated at CDS, Strasbourg, France. JK and RW acknowledge support from DFG, Germany, grant KR 1053/5. PHH acknowledges partial support from NSF grant AST-9720704, NASA ATP grant NAG 5-3018 and LTSA grant NAG 5-3619 to the University of Georgia. Quite a number of mosquitoes were killed during the preparation of this manuscript.

REFERENCES

Alcalá J. M., Krautter J., Schmitt J. H. M. M., Covino E., Wichmann R., Mundt R., 1995, *A&AS*, 114, 109
 Alcalá J. M. et al., 1996, *A&AS*, 119, 7
 Basri G., Martin E. L., Bertout C., 1991, *A&A*, 252, 625
 Bouvier J., 1990, *AJ*, 99, 946
 Bouvier J., Bertout C., Benz W., Mayor M., 1986, *A&A*, 165, 110
 Briceño C., Hartmann L. W., Stauffer J. R., Gagne M., Stern R. A., 1997, *AJ*, 113, 740
 Calvet N., Hartmann L., 1992, *ApJ*, 386, 239
 Comerón F., Torra J., Gómez A. E., 1994, *A&A*, 286, 789

Covino E., Alcalá J. M., Allain S., Bouvier L., Terranegra L., Krautter J., 1997, *A&A*, 328, 187
 Dame T. M. et al., 1987, *ApJ*, 322, 706
 Dubath P., Reipurth B., Mayor M., 1996, *A&A*, 308, 107
 Falgarone E., Puget J. L., 1986, *A&A*, 162, 235
 Favata F., Barbera M., Micela G., Sciortino S., 1993, *A&A*, 277, 428
 Feigelson E. D., 1996, *ApJ*, 468, 306
 Frink S., Röser S., Neuhäuser R., Sterzik M. F., 1997, *A&A*, 325, 613
 Gould B. A., 1879, in Corni P. E., ed., *Uranometria Argentina*. Impr. de P. E. Corni, Buenos Aires, p. 355
 Guillot P., Sterzik M. F., Schmitt J. H. M. M., Motch C., Egret D., Voges W., Neuhäuser R., 1998, *A&A*, 334, 540
 Hartmann L. W., Stauffer J. R., 1989, *AJ*, 97, 873
 Hartmann L. W., Soderblom D. R., Stauffer J. R., 1987, *AJ*, 93, 907
 Hartmann L., Hewett R., Calvet N., 1994, *ApJ*, 426, 669
 Hauschildt P. H., Allard F., Baron E., 1999, *ApJ*, 512, 377
 Houdebine E. R., Stempels H. C., 1997, *A&A*, 326, 1143
 Hughes J., Hartigan P., Clampitt L., 1993, *AJ*, 104, 680
 Hughes J., Hartigan P., Krautter J., Kelemen J., 1994, *AJ*, 108, 1071
 Jones B. F., Fischer D. A., Stauffer J. R., 1996, *AJ*, 112, 1562
 Krautter J., 1991, in Reipurth B., ed., *ESO Rep. 11, Low Mass Star Formation in Southern Molecular Clouds*, p. 127
 Krautter J., Wichmann R., Schmitt J. H. M. M., Alcalá J. M., Neuhäuser R., Terranegra L., 1997, *A&AS*, 123, 329
 Krautter J., Bastian U., 1980, *A&A*, 88, L6
 Magazzù A., Rebolo R., Pavlenko Y. V., 1992, *ApJ*, 392, 159
 Magazzù A., Martin E. L., Sterzik M. F., Neuhäuser R., Covino E., Alcalá J. M., 1997, *A&AS*, 124, 449
 Martin E. L., Rebolo R., Magazzù A., Pavlenko Y. V., 1994, *A&A*, 282, 503
 Micela G., Favata F., Sciortino S., 1997, *A&A*, 326, 221
 Mitskevich A. S., Natta A., Grinin V. P., 1993, *ApJ*, 404, 751
 Mizuno A. et al., 1998, *ApJ*, 507, L83
 Murphy D. C., Cohen R., May J., 1986, *A&A*, 167, 234
 Neuhäuser R., Brandner W., 1998, *A&A*, 330, L29
 Neuhäuser R., Sterzik M. F., Torres G., Martin E. L., 1995, *A&A*, 299, L13
 Neuhäuser R., Torres G., Sterzik M. F., Randich S., 1997, *A&A*, 325, 674
 Palla F., Galli D., 1997, *ApJ*, 476, L35
 Panagi P. M., Byrne P. B., Houdebine E. R., 1991, *A&AS*, 90, 427
 Pöppel W., 1997, *Fundam. Cosmic Phys.*, 18, 1
 Reipurth B., Pedrosa A., Lago M.T.V.T., 1996, *A&AS*, 120, 229
 Silk J., 1985, in Lucas R., Omont A., Stora R., eds, *Birth and Infancy of Stars*. Elsevier, Amsterdam, p. 349
 Soderblom D. R., Jones B. F., Balachandran S., Stauffer J. R., Duncan D. K., Fedele S. B., Hudon J. D., 1993, *AJ*, 106, 1059
 Stauffer J. R., Hartmann L. W., 1987, *ApJ*, 318, 337
 Stauffer J. R., Hartmann L. W., Soderblom D. R., Burnham N., 1984, *ApJ*, 280, 202
 Wichmann R., Krautter J., Schmitt J. H. M. M. et al., 1996, *A&A*, 312, 439
 Wichmann R., Krautter J., Covino E., Alcalá J. M., Neuhäuser R., Schmitt J. H. M. M., 1997a, *A&A*, 320, 185
 Wichmann R., Sterzik M., Krautter J., Metanomski A., Voges W., 1997b, *A&A*, 326, 211
 Wichmann R., Bouvier J., Allain S., Krautter J., 1998a, *A&A*, 330, 521
 Wichmann R., Bastian U., Krautter J., Jankovics I., Ruciński S. M., 1998b, *MNRAS*, 301, L39

This paper has been typeset from a \TeX/L\AA\TeX file prepared by the author.